ADMITTANCE RESPONSE OF PZT TRANSDUCERS BONDED TO A STRUCTURAL MEMBER SUBJECTED TO EXTERNAL LOADING

[1]Akshay S. K. Naidu, [2]Karthik Reddy Awala
[1]Associate Professor, [2]Research Student
Department of Civil Engineering,
Methodist College of Engineering and Technology, Hyderabad, India 500001

Abstract*—In the Electro Mechanical Impedance method (EMI) for structural health monitoring (SHM), a piezoelectric ceramic transducer (PZT) is bonded on to the structure to be regularly monitored. There exists a dynamic coupling between the mechanical impedance of the structure and the mechanical impedance of the bonded PZT transducer, which is reflected in the electrical admittance response of the PZT to frequency of its actuation, popularly called as the admittance signature. Damage or deterioration in the structure affects the mass, stiffness and damping parameters locally, which alters the mechanical impedance of the structure. This change reflects in the admittance signature of the PZT transducer by which the structural health can be assessed. External loads can also induce mass and stiffness changes locally and thus alter the admittance signature. The load induced changes in the admittance signatures have to be filtered out to get factual damage induced changes for reliable SHM. This paper presents the results of a numerical study, carried out to understand the influence of external loading on the PZT admittance signature, using coupled field FE analysis in ANSYS™.

***Index Terms*—Electromechanical Impedance (EMI), Piezoelectric transducers, Lead Zirconate Titanate (PZT), Structural Health Monitoring (SHM), Admittance Signatures, Coupled Field FE Analysis. (key words)**

I. INTRODUCTION

The structures performance assessment in terms of its service life, durability, sustaining any failure conditions has always been important criteria. The purpose of the early detection of the defects in the structures is to ensure that the structure does not disintegrate and extends its service life without much efforts investing in repairs. The conventional methods of the structural condition assessment by visual inspections and localized NDT techniques are inefficient for determining incipient damages and give early warning to the user. Especially for massive public structures, to ensure structural integrity and safety, it is essential to continuously monitor the structure at periodic intervals without much human interference. Thus, the concept of structural health monitoring (SHM) is conceived [1].

The SHM process involves (a) generation of diagnostic signals, by using passive or active sensors mounted at critical locations of the structure, (b) transmission of the signals through reliable electronic communication systems without deterioration and noise (c) analysis of the diagnostic signal to derive meaningful assessment criteria for the structure (d) structural damage and assessment metric to quantify the damage and (e) generating an alarm to give timely warning to the user. SHM technology aims at full automation of all these components without active human interference [2], [3]. Extensive research is being carried out throughout the world to achieve this goal of the SHM philosophy. Numerous techniques in SHM have been developed in each of these components [4].

The electromechanical impedance (EMI) method which utilizes the electric impedance characteristics of the piezoelectric ceramic transducers bonded to the structure has potential applications for structural health monitoring technology. Piezoelectric materials deform (strain) when an electric field is applied across their electrodes and conversely produce voltage across their electrodes due to an applied mechanical strain. This phenomenon is most prominently observed in piezoelectric ceramics, such as Lead Zirconate Titanate (PZT). This bifunctional property makes the PZT be used both as actuators and sensors. Many methods involving the PZT transducer chips use two chips, one as an actuator to generate a wave and the other as a receiver to sensor the incident wave for diagnosis. However, in the EMI method, a single PZT transducer is used to simultaneously actuate and sense the signal. Thus, in the EMI technique, the PZTs are used as self-sensing actuators [5].

To assess the structure, the diagnostic signal generated in the EMI method is the admittance signature of the PZT transducer surface-bonded to the structure, or sometimes, embedded within the concrete matrix of a structural element. The admittance signature is the electrical admittance of the PZT over a frequency range of excitation, which shall be elaborated more in the next section. Occurrence of damages in the structure, changes the pattern of the admittance signature of the PZT which is in the vicinity of the damage location. Numerous proof-of-the-concept tests have been successfully reported, and many of the technical aspects for implementation of this technique have been investigated over the past two decades[5]–[7].

For research purposes, towards understanding of the technical parameters involved in the EMI technique, many analytical or semi-analytical models have been derived and tested against the experimental investigations [8], [9]. Researchers have also demonstrated that the EMI technique can be numerically simulated by adopting the coupled field finite element analysis in ANSYS™ [9], [10]. Using this numerical simulation, the admittance signatures can be directly obtained just as we get in the experimental results. Further, by adjusting the various parameters, particularly damping parameters, a close match of the pattern of admittance signatures generated numerically with the experimentally generated signatures, has been achieved [10]. Thus, the coupled field FE simulations help in investigating the EMI technique without the need of complex experimental set-up.

In this paper, the coupled field FE analysis of the EMI technique is adopted to study the influence of loading on the admittance signature. This is so as to differentiate the admittance signature changes due to the presence of excessive load and load induced stresses, as opposed to those due to factual damages in the structure. The FE models are chosen to study the effect of induced longitudinal stresses and flexural stresses on the admittance signatures of the PZT transducer.

II. METHODOLOGY

Electromechanical Impedance Method

In the electromechanical impedance (EMI) method, the PZT transducer is excited through an alternating voltage signal using an impedance analyzer or an LCR meter, over a frequency range within 10 - 200 kHz. This induces a high frequency vibration in the PZT. The PZT, which is surface-bonded onto or embedded within the structural element, induces actuation in the structure, locally. The PZT actuates the structure at any particular frequency and the structural response is simultaneously sensed by the PZT. If the bond between the PZT and the structure is strong, there exists a coupling between the mechanical impedance of the structure and the mechanical impedance of the PZT. This coupling is reflected in the electrical admittance response of the bonded PZT at each frequency. The frequency response curve or the admittance response versus the excitation frequency range is called as the electromechanical admittance signature. The electromechanical admittance of the PZT is measured directly by the impedance measuring instrument, such as the impedance analyzer (HP 4192/4194 A) or an LCR meter (Agilent E4980A Precision LCR meter) [3], [11].

Any damage, such as a crack, debond or corrosion in the structure, alters the mass, stiffness and damping parameters locally around the damage. The mechanical impedance of the structure is dependent on the mass, stiffness and damping parameters. Thus, any damage alters the mechanical impedance of the structure locally, in the near vicinity of the damage location. Due to the impedance coupling that exists between the PZT and the structure, the changes in mechanical impedance reflects in the change in the electrical admittance of the PZT attached to the structure. Thus, change in the pattern of the admittance signature serves as the damage indicator. The changes in the admittance signatures can be statistically quantified or measured by parameter-based damage metrics [3], [11].

Numerical Simulation

Many analytical models in 1D, 2D and 3D have been developed for the EMI impedance techniques and experimentally verified. A summary of these models and their resultant equations can be obtained in the literature [5], [9], [12].

The analytical models, however, are limited to simple structures with simple geometries and boundary conditions. When the structure to be studied is relatively complex or with complicated boundary conditions, or when the targeted model involves a system of structures interacting with each other, analytical modeling is usually impossible.

Numerical models turn up to be a viable option, which often provide close enough approximation to the exact solution, satisfactory for engineering applications. Recent developments of various finite element method (FEM) based software package and advancement in computer hardware render the numerical modeling technique more attractive option.

Researchers have proposed a semi-analytical modeling approach incorporating the FE model and the impedance based model, commonly known as finite element analysis (FEA)-based impedance model. This model enables the modeling of PZT-structure interaction without the presence of PZT patch in the model, as it has been simplified and represented by a force or moment. This approach retains the simplicity of the impedance based model while utilizes the strength of FEM including the ability in modeling generic distributed structures possessing anisotropic material, mass loading and non-uniform boundary conditions.

Liu and Giurgiutiu [13] compared the real part of the impedance from both the FEA-based impedance model (non-coupled) and coupled field model of a 1-D narrow beam structure to those of the experimental tests. The coupled field model exhibited closer agreement to the experimental results.

Yang and co-researchers [9] studied the ability of coupled-field FE model in simulating the PZT-structure interaction. PZT patch surface-bonded onto aluminium structures of various shapes were simulated and compared with the experimental counterparts. The overall outcome of the numerical simulation showed excellent agreement with the experimental tests up to a frequency as high as 1000 kHz.

Advantages of FE simulation using coupled elements include: results in terms of electrical admittance can be readily obtained and compared with the experimental counterparts, higher accuracy can be achieved as the entire PZT patch can be simulated instead of being replaced by a force or moment, local modes omitted in the analytical model can be excited in the coupled field model, and the bonding layer and shear lag effect can be physically simulated.

Lim and Soh [10] showed that by adjusting material parameters and choosing an appropriate Damping Model the results obtained from the couple field. FE Simulations can have very close arrangement with the experimentally obtained signatures.

In this work we adopted the simulation method by using Lim and Soh [10].

Coupled Field Finite Element Simulation

In ANSYS™, piezoelectric analysis comes under the category of coupled field analysis. Coupled-field analysis considers the interaction or coupling between two or more disciplines of engineering. Piezoelectric analysis caters for the interaction between structural and electric fields.

Coupled-field analysis derives solutions to problems not possible with the usual FEM, by simplifying the modeling of coupled-field problems. Piezoelectric analysis makes use of direct coupling method, which involves only one analysis with the use of one coupled-field element containing all necessary degrees of freedom.

This formulation is very convenient for evaluating the admittance signatures used in the EMI technique. The complex electrical admittance signature, which is the ratio of electric current to voltage, can be expressed as:

$$\bar{Y} = \frac{\bar{I}}{\bar{V}}$$

where $\bar{Y}$ is complex electrical admittance of the PZT, $\bar{V}$ is the sinusoidal voltage applied and $\bar{I}$ is the modulated current in the PZT, with the bars above indicating complex terms. When the voltage is taken as $\bar{V} = 1 + 0i$, the output current directly gives the electrical admittance.

By performing Harmonic Analysis and extracting the current as output we can obtain the admittance signature. The details of the steps involved in modeling and harmonic analysis were similar to those used in the literature [10], [14].

III. FE SIMULATIONS AND CASES

Two simple models are considered in this study with the aim of understanding the influence of loading on the admittance signatures. A prismatic member is considered of dimensions: L= 0.3 m; b = 0.02m; h = 0.002m {30cm x 2cm x 0.2cm}.

Two cases of loading are considered:

a) Axially loaded member: Fixed support at the top of the member, which is acting under gravity and subjected to loading at the bottom. The loading is simulated by varying the density at the last 1 cm strip of the beam. The densities were increased to a limit below the yield

strength of the material. This beam would experience axial stresses. The PZT is located at one-third of the length of the member and at the center of the width, as shown in Figure 1(a).

b) Simply supported beam subjected to flexural stress: The same prismatic member is subjected to flexural loading. The load is induced by placing a block of mass at the centre of the span. Increasing the densities of the mass simulates increase in the load. Two PZTs are bonded at 1/3rd length from the end, one on top layer which can determine the compression stresses and one at the bottom layer for determining the tensile stresses. Densities for the mass block are varied below the yield strength of the material of the beam. This beam would experience flexural stresses. The illustrations are shown in Figure 1(b).

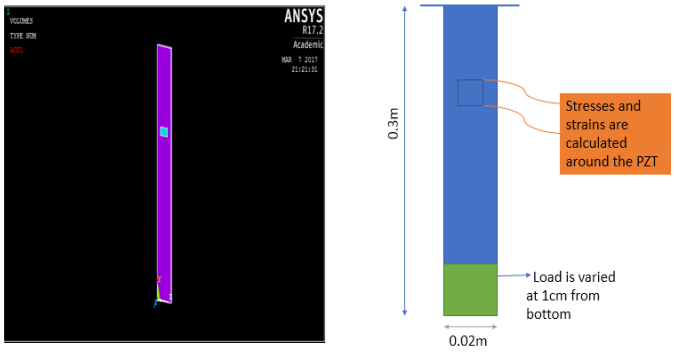

(a) Axial loading on a prismatic member

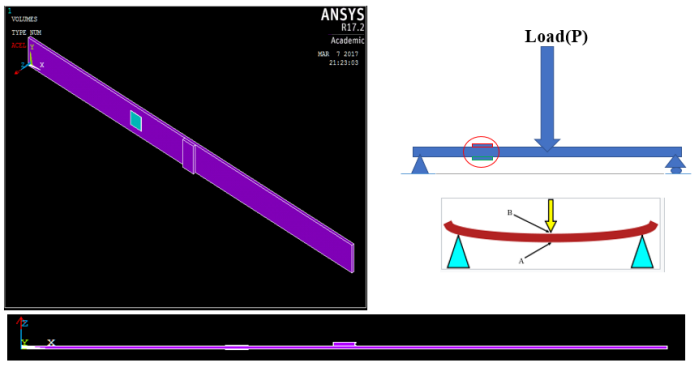

(b) Flexural loading on a beam member

Figure 1 Ansys Modelling of the (a) Axial Load on the Member (b) Flexural Load on the Member

Details of the FE model

Some features of the FE model are as follows:

Element Types Used:

(a) Solid 45 for material of the beam:

This is a 3D 8-noded brick element having three degrees of freedom at each node: translations in the nodal x, y, and z directions.

(b) Solid 45 for piezoelectric material:

This is a 3D 8-noded coupled field element with multi-physics capabilities in particular piezoelectric properties.

Material Properties

(a) Structural Material Properties: The material used for the prismatic member or the beam was metallic with the following material properties as given in Table 1.

Table 1 Properties for the Structural Material

Property	**Notation & Value**
Young's Modulus	$E = 6.89 \times 10^{10}$ N/m^2
Density	$\rho = 2600$ kg/m^3
Poisson's ratio	$\nu = 0.3$
Hysteretic damping ratio	$\xi = 0.0005$

(b) Piezoelectric Material Properties: The material used for the PZT is based of PI 155 of the PI Ceramic, a German company, which has been used by earlier researchers, with the following material properties as given in Table 2

Table 2 Properties for the PZT material

Parameters	**Symbols**	**Values**	**Units**
Density	ρ	7800	kg/m^3
Compliance	$s_{11} = s_{22}$	15	10^{-12} m^2/N
	s_{33}	19	
	$s_{12} = s_{21}$	-4.5	
	$s_{13} = s_{31}$	-5.7	
	$s_{23} = s_{32}$	-5.7	

	$s_{44}= s_{55}$	39	
	s_{66}	49.4	
Electric permittivity	ε^T_{11}	1980	
(Relative values)	ε^T_{22}	1980	
	ε^T_{33}	2400	
Piezoelectric strain coefficients	d_{31}	-210	10^{-12} C/N
	d_{32}	-210	
	d_{33}	500	
	d_{24}	-	
	d_{15}	580	
Mechanical quality factor	Q_m	100	
Damping ratio (Hysteretic)	$\xi_{PZT} = (2Q_m)^{-1}$	0.005	

FE Meshing

Mesh used: Hexagonal meshing type. Cube shaped meshes of dimension 1 mm. Both the PZT and the structural beam were meshed with the same mesh for compatibility.

Loading

As presented earlier, long prismatic beam subjected to axial loading and a simply supported beam subjected to flexural loading are considered for this numerical study.

The axial load in the cantilever beam is induced by increasing the density of the bottom segment of the beam, which is subjected to gravity. Whereas, in simply supported beam, flexural load is induced by placing a mass block at the center, and increasing the density of that block. The thickness of the block is taken as h, same as the thickness of the beam. The width of the block is same as the width

Thus, the various values of densities to increase the mass of the block for simulating loading are as follows in Table 3:

Table 3 Load Cases Considered in terms of densities of the loading block

Load Case	1	2	3	4	5
Density (in kg/m^3)	2600	10000	25000	50000	75000

The maximum limit for the densities is calculated from the yield point as follows:

Bending equation,

$$\frac{M}{I} = \frac{f}{y} = \frac{E}{R} \quad (1)$$

where,

M = bending moment; I = moment of inertia; f = bending stress; E= Young's modulus; R= radius of curvature; y = perpendicular distance from the neutral axis;

Consider,

$$M = \frac{I}{y} f = Z f_{\max} = \frac{bd^2}{6} f_{\max} \quad (2)$$

$$f_{\max} = \frac{6M}{bd^2} \le f_y \quad (3)$$

Equating to the extreme value to the yield point, and writing the bending moment M, in terms of the density ρ and dimensions of the loading block, we get

$$\rho \le \frac{2}{3} \frac{f_y}{Lhg} bd^2 \quad (4)$$

Taking the yield point of Aluminium from standard values of the texts, the density was calculated and the maximum limit was restricted to the above below.

$$\rho = 75025 \text{ kg/m}^3 \quad (5)$$

This is done to ensure that the flexural loading stresses the beam within its elastic limit of the material of the beam.

Analysis Types

Three different analyses were performed:

(i) Static analysis: This was done to calculate the stresses and strains developed in the beam at the location where the PZT is bonded. Three points under the beam were selected, two at the edges and one at the centre, and the stresses and strains were noted at these points an average was calculated.

(ii) Modal analysis: This was done to identify the natural frequencies of the beam mounted with the PZT, and to study the changes in the natural frequencies due to changes in the load condition. First twenty modal frequencies were considered for this purpose and compared. Block Lancoz eigen value extraction method was adopted in ANSYS™.

(iii) Harmonic analysis: The harmonic signature of admittance (real or imaginary) vs frequency is what is typically obtained in a real experimental set-up. Studying the changes in the harmonic admittance signature with various load cases is the key objective for the purposes of Structural Health Monitoring. The peaks in the signatures obtained from Harmonic analysis occur at points, corresponding to the natural frequencies of the system. Changes in the location of the peak in these signatures, are indicative of natural frequency shifts, which in turn gives insight into structural integrity.

IV. Results and Discussion

For Axial Loading Case

Static Analysis:

Static analysis was used for correlating load conditions to stresses developed below the PZT transducer in structural components caused by only steady-state inertial forces such as gravity. The axial stresses increase in magnitude as shown in Figure 2.

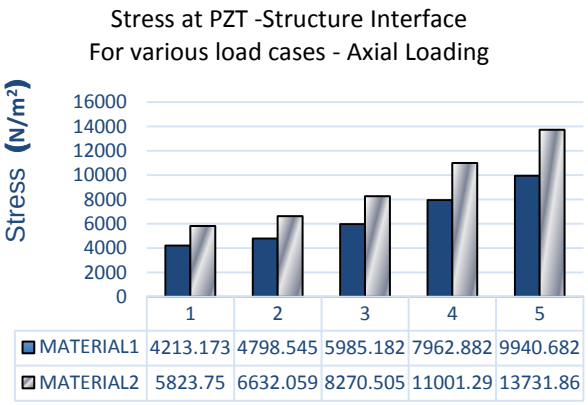

Figure 2: Axial stresses in the prismatic member at the PZT bottom – structure interface
Material 1 is for the PZT and Material 2 is the structural material (Aluminium)

Modal Analysis:

Modal frequency for any structure is certain natural frequency at which it vibrates freely without any external force. It is observed that natural frequency reduces when the load increases. The values of the first 20 modal frequencies for various loads is presented in Table 4. It can be noted for the same amount of load the changes in frequency in the higher modes is greater. This change in the frequencies of load cases 2, 3, 4 and 5 as compared with the load case 1 (which is the case of no external load) is shown in Table 5. Higher frequency modes are capable of notifying any changes or damages in the structure more effectively as compared to the lower frequency modes. As EMI method typically operates in the order of kHz, it is very sensitive in detecting even small changes.

Table 4 Natural Frequencies of the member with PZT for various axial loading cases

	Load Cases (as per Table 3)				
	1	2	3	4	5
Mode	Structural Natural Frequencies (in Hz)				
1	18.6	15.9	12.8	10.2	8.7
2	116.0	104.0	95.3	90.4	85.9
3	184.4	157.9	127.0	100.6	88.4
4	325.0	299.4	285.3	278.6	275.7
5	526.8	480.9	412.3	340.9	296.4
6	638.2	599.2	581.2	572.2	567.7
7	1055.7	1004.0	928.1	879.7	858.7
8	1126.8	1013.1	981.9	968.6	959.8
9	1572.6	1446.4	1306.9	1213.4	1172.9
10	1577.8	1513.9	1485.8	1463.5	1445.0
11	2205.6	2129.7	2091.8	2052.1	2014.9
12	2650.1	2457.8	2309.9	2237.9	2210.5
13	2938.2	2819.0	2679.8	2602.4	2430.9
14	3055.0	2849.6	2795.7	2726.0	2561.7
15	3742.2	3516.8	3372.0	2793.6	2660.2
16	3776.3	3672.7	3386.4	3329.2	3304.8
17	4291.9	3925.2	3594.0	3480.1	3383.4
18	4719.4	4571.3	4456.3	4315.6	4201.1
19	4819.4	4597.6	4480.6	4401.5	4366.7
20	5767.9	5436.9	5243.9	5104.9	5000.9

Table 5: Natural Frequency reduction values of the structure for load cases as compared to the first load case (axial loading).

	Load Cases (as per Table 3)			
Mode	2	3	4	5
	Frequency Reductions (in Hz)			
1	2.7	5.8	8.5	10.0
2	11.9	20.7	25.6	30.1
3	26.5	57.4	83.7	95.9
4	25.5	39.6	46.4	49.2
5	45.9	114.5	185.9	230.5
6	39.0	57.0	66.0	70.5
7	51.7	127.6	176.0	197.0
8	113.7	144.9	158.2	167.0
9	126.2	265.7	359.2	399.7
10	63.9	92.0	114.3	132.8
11	75.9	113.8	153.5	190.7
12	192.3	340.2	412.2	439.6
13	119.2	258.4	335.8	507.3
14	205.4	259.3	329.0	493.3
15	225.4	370.2	948.6	1082.0
16	103.6	389.9	447.1	471.5
17	366.7	697.9	811.8	908.5
18	148.1	263.1	403.8	518.3
19	221.8	338.8	417.9	452.7
20	331.0	524.0	663.0	767.0

Harmonic Analysis:

Harmonic response analysis gives the forced vibration response of the electrical admittance of the surface-bonded PZT transducer with the exciting frequency. The idea is to calculate the structures response at several frequencies (0 to 5 kHz) and obtain a graph of some response quantities versus frequency. We considered the real admittance (conductance) versus frequency, as this is the most commonaly used in the EMI method.

From these conductance signatures, the "peak" responses are then identified on these graphs for further study analysis. The peaks correspond to the resonance of the exiciting frequency with the structural natural frequency. Thus, the frequencies of the peaks can be correlated with the natural frequencies in the Table 4. The conductance signatures are extracted from 0-5000 Hz frequency values. For clear and a closer view representation, few sets of the graphs of conductance signatures are considered over a limited frequency range. Figure 3 shows the conductance signature for axially loaded prismatic member for the frequency range of 1400 – 1600 kHz. Figure 4 shows the conductance signature for axially loaded prismatic member for the frequency range of 1400 – 1600 kHz.

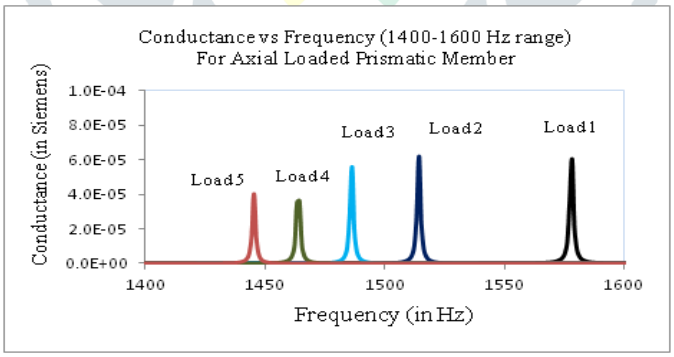

Figure 3: Conductance Signature for axially loaded prismatic member (1400-1600 Hz frequency range)

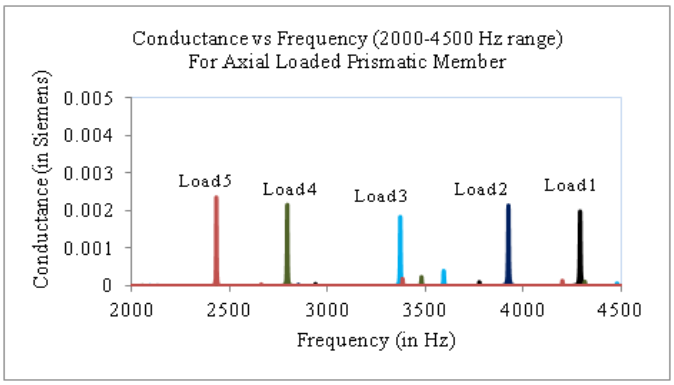

Figure 4: Conductance Signature for axially loaded prismatic member (2000-4500 Hz frequency range)

From both the figures, we can observe that with increase in load the conductance signatures shift leftwards, that is for the same mode the natural frequency values of the structure are reducing. These natural frequencies correspond to the peaks in the conductance signature. From the basic structural dynamics, we know that the natural frequency of a system is directly proportional to the square rooot of the stiffness and is inversely proportional to the square rooot of the lumped mass. Although the load increases the axial stress in the member, and tends to increase the dynamic stiffness, the natural frequencies do not increase. Here the load is induced by increasing the mass and not just applying the force. Thus, with increase in mass the natural frequencies reduce in values. This trend shown here is opposed to the trends seen in the works of [15]–[17].

For Flexural Loading Case

In similar lines as in the axial loading case, the flexural loading case results are also observed.

Static Analysis:

From static analysis, the stresses developed at the PZT-structure interface, both on the PZT transducer and the structure, are observed. In this case, however, there are two PZTs, one on the compression layer and the other on the tension layer. The axial stresses developed at the PZT-structure interface for both these cases are shown in Figures 5 and 6, respectively. Clearly, the magnitude of flexural stresses in increasing with the increase in the load.

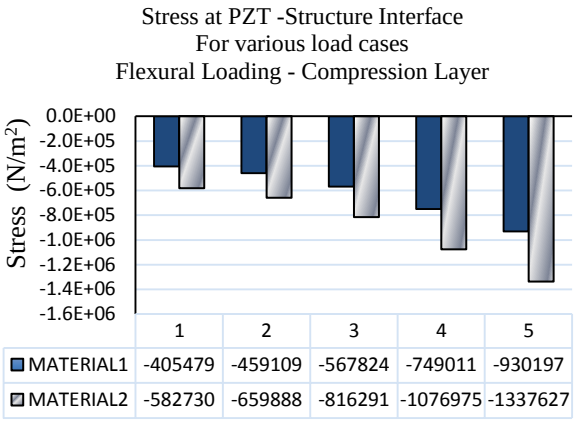

Figure 5: Flexural stresses in the compression layer of the simply supported beam member at the PZT – Structure Interface for various load cases Material 1 is for the PZT and Material 2 is the structural material (Aluminium)

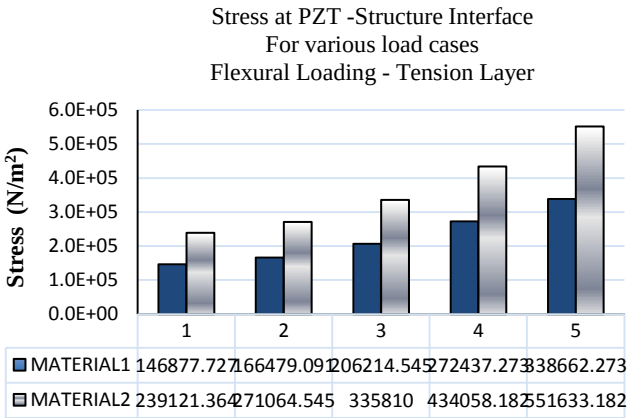

Figure 6: Flexural stresses in the tension layer of the simply supported beam member at the PZT – Structure Interface for various load cases Material 1 is for the PZT and Material 2 is the structural material (Aluminium)

Although the signs of the stresses are different in both the cases of compression and tension, as expected, we can see the increase in the magnitudes of the stresses in both the cases with the increase in loading. Another, observation is that the magnitudes of the compressive and tensile stresses are different, which is usually not the case in flexural stresses in beams. This might be due to the difference in the stiffness effects produced by the PZT under tension and in compression. This, however, is not fully understood and needs further investigation.

Modal Analysis:

Similar to the axial loading case, the modal analysis results for the flexurally loaded simply supported beam is presented herein. It is again observed that natural frequency reduces when the load increases. The values of the first 20 modal frequencies for various loads is presented in Table 6. It can be again noted that for the same amount of load the changes in frequency in the higher modes is greater. This change in the frequencies of load cases 2, 3, 4 and 5 as compared with the load case 1 (which is the case of no external load) is shown in Table 7. In some cases such as mode numbers 2, 4, 8, 9 and 11, and so on, we find that the frequency reduction values are extremely less compared to the other modes. This is because of the presence of vibrational nodes at the location of the load, either in the flexural or torsional modes of vibration. These observations are also helpful in identifying damage locations [3].

Table 6: Natural Frequencies of the member with PZT for various axial loading cases

	Load Cases as per Table 3				
	1	2	3	4	5
Mode	Structural Natural Frequencies (in Hz)				
1	81.718	75.044	65.324	55.091	48.513
2	207.17	207.09	206.92	206.64	206.37
3	512.83	484.86	453.96	430.45	418.92
4	829.09	826.75	732.75	599.09	517.14
5	908.56	846.64	787.99	675.1	601.75
6	1027	916.53	822.01	814.09	806.18
7	1361.9	1303	1249.3	1215.1	1200
8	1867.6	1861.4	1848.8	1827	1804.5
9	2152.4	2151.9	2150.8	2149	2147.1
10	2619.1	2528.6	2457.8	2417.5	2400.8
11	2682.4	2677.3	2654.9	2494	2418.9
12	3093.4	2882.1	2667.2	2650.4	2633.7
13	3304.6	3264.8	3179.9	3031.9	2887.3
14	4331.4	4212.9	4129.7	4085.5	4021.3
15	4438.9	4436.9	4279.2	4106.2	4067.7
16	4854.2	4540	4434.7	4429	4423.1
17	5133.9	5096.4	4977.7	4814.1	4653.8
18	5440.5	5214.9	5019.1	4888.6	4741.9
19	6425.9	6279.5	5826.5	5089.8	4778.9
20	6871.3	6532	6185.6	6137.9	6118.7

Table 7: Natural Frequency reduction values of the structure for load cases as compared to the first load case (flexural loading).

	Load Cases (as per Table 3)			
	2	3	4	5
Mode	Frequency Reductions (in Hz)			
1	6.7	16.4	26.6	33.2
2	0.1	0.3	0.5	0.8
3	28.0	58.9	82.4	93.9
4	2.3	96.3	230.0	312.0
5	61.9	120.6	233.5	306.8
6	110.5	205.0	212.9	220.8
7	58.9	112.6	146.8	161.9
8	6.2	18.8	40.6	63.1
9	0.5	1.6	3.4	5.3
10	90.5	161.3	201.6	218.3
11	5.1	27.5	188.4	263.5
12	211.3	426.2	443.0	459.7
13	39.8	124.7	272.7	417.3
14	118.5	201.7	245.9	310.1
15	2.0	159.7	332.7	371.2
16	314.2	419.5	425.2	431.1
17	37.5	156.2	319.8	480.1
18	225.6	421.4	551.9	698.6
19	146.4	599.4	1336.1	1647.0
20	339.3	685.7	733.4	752.6

Harmonic Analysis:

The conductance signatures obtained for the PZTs located in the compression layer and the tension layer, for a small frequency range of 2800-3400 Hz, is shown in Figures 7 and 8, respectively. The frequencies of the peaks can be correlated with the natural frequencies in the Table 6. The conductance signatures are extracted from 0-5000 Hz frequency values.

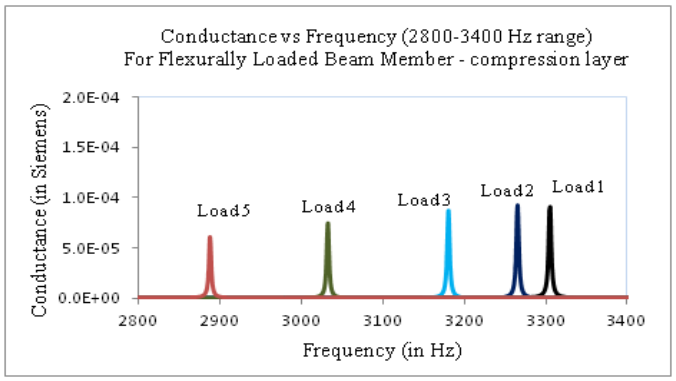

Figure 7: Conductance Signature for flexurally loaded simply supported beam member for PZT in the compression layer (2800-3400 Hz frequency range)

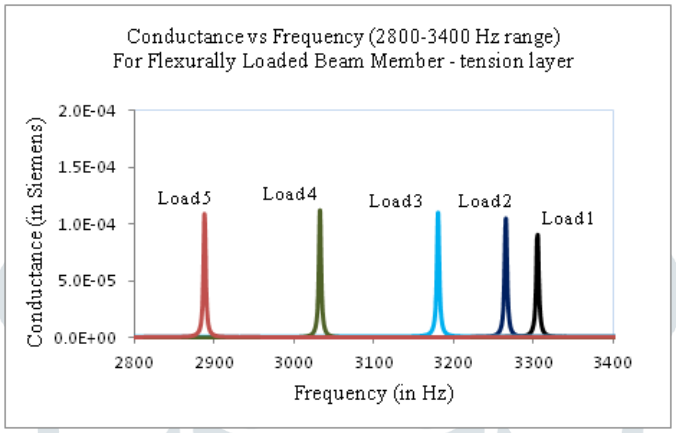

Figure 8: Conductance Signature for flexurally loaded simply supported beam member for PZT in the tension layer (2800-3400 Hz frequency range)

From both the figures, it can be observed that with increase in load the conductance signatures shift leftwards, that is for the same mode the natural frequency values of the structure are reducing. The values of the peaks seam to decrease in the compression zone while these peak values seem to increase in the tension zone. The values of the peaks are closely related to the damping parameters locally, study and discussion of which is beyond the scope of this work.

Again we observe that as the load increases the flexural stresses in the member, the natural frequencies do not increase, rather thet decrease. Again, the load is induced by increasing the mass and not just applying the force. Thus, with increase in mass the natural frequencies reduce in values. This trend shown here is opposed to the trends seen in the previous works as aforementioned.

It is also note that the compression and tension zone give same pattern shifts, that the frequency reduction values is the same. Thus, by this analysis presented in this paper, the compressive or tensile nature of the stresses cannot be distinguish using the PZT admittance signatures.

It may be noted that on occurrence of a damage the pattern of frequency shifts for various modes is not uniform, as it can be seen in the case of the pattern seen for the loading case[11], [18]. This difference can be utilized for identifying pattern changes for induced load versus factural; structural damage cases.

V. CONCLUSIONS

In this work, the coupled field FE modeling of the EMI technique is adopted to study the influence of loading on the admittance signature. The FE models of a prismatic member are chosen with axial and flexural loading to study the effect of induced longitudinal stresses and flexural stresses on the admittance signatures of the PZT transducer bonded on to the member.

For both the models, as load is increased, the resultant stress increased at the PZT-structure interface. An important observation is that for the same amount of load, the higher modes result in a larger frequency reduction shifts when compared to the lower modes. This result concurs with the findings of the previous researchers that the higher frequency modes are more sensitive to changes in the structural parameters. Thus, the EMI technique using PZT sensors, which typically operates at ultrasonic frequencies actuating the higher modal frequencies, is more sensitive for SHM purposes than the conventional vibration based NDT methods, where only the first three or four modes are only considered.

Usually, we may expect that axial load will increase the stiffness of a structural member and thus, natural frequencies may increase. However, as loads are induced by gravity applied on the mass blocks, increase in the mass results is decrease in frequencies, as observed in this investigation. Thus, it can be said that the structural member response is dominated by mass over the stiffness parameter.

In the case of flexural loading, since the load is concentrated at the center and applied on the top surface, the stresses on the top compression layer was observed to be higher compared to the bottom tension layer. In modal analysis, we observe that for certain modes there are negligible natural frequency shifts with increasing loads. This is because for those modes, the vibration nodes (points of zero displacement) coincide with the position of load. resulting in low frequency shifts.

For the same loading condition, the shift in compression and tension have similar peak pattern. Essential conclusion is that natural frequencies correlate with the stresses, but does not indicate whether the beam surface is in compression or in tension.

The results presented in this paper shall be useful to the researchers who would be interested in further analysis of the EMI method, especially in the area of pattern recognition of the changes in the admittance signatures due to structural damage identification and induced stress.

REFERENCES

[1] C. R. Farrar and K. Worden, "An introduction to structural health monitoring," *Philos. Trans. R. Soc. Lond. Math. Phys. Eng. Sci.*, vol. 365, no. 1851, pp. 303–315, 2007.

[2] S. Bhalla, "Smart system based automated health monitoring of structures," M.Engg. Thesis, Nanyang Technological University, Singapore, 2001.

[3] A. S. K. Naidu, "Structural damage identification with admittance signatures of smart PZT transducers.," PhD Thesis, Nanyang Technological University, Singapore, 2004.

[4] H. Sohn *et al.*, *A review of structural health monitoring literature: 1996-2001*. Los Alamos National Laboratory Los Alamos, NM, 2004.

[5] V. G. M. Annamdas and C. K. Soh, "Application of electromechanical impedance technique for engineering structures: review and future issues," *J. Intell. Mater. Syst. Struct.*, vol. 21, no. 1, pp. 41–59, 2010.

[6] G. Park, H. Sohn, C. R. Farrar, and D. J. Inman, "Overview of piezoelectric impedance-based health monitoring and path forward," *Shock Vib. Dig.*, vol. 35, no. 6, pp. 451–464, 2003.

[7] V. G. Annamdas and M. A. Radhika, "Electromechanical impedance of piezoelectric transducers for monitoring metallic and non-metallic structures: A review of wired, wireless and energy-harvesting methods," *J. Intell. Mater. Syst. Struct.*, vol. 24, no. 9, pp. 1021–1042, 2013.

[8] Y. Yang, Y. Y. Lim, and C. K. Soh, "Practical issues related to the application of the electromechanical impedance technique in the structural health monitoring of civil structures: I. Experiment," *Smart Mater. Struct.*, vol. 17, no. 3, p. 35008, 2008.

[9] Y. Yang, Y. Y. Lim, and C. K. Soh, "Practical issues related to the application of the electromechanical impedance technique in the structural health monitoring of civil structures: II. Numerical verification," *Smart Mater. Struct.*, vol. 17, no. 3, p. 35009, 2008.

[10] Y. Y. Lim and C. K. Soh, "Towards more accurate numerical modeling of impedance based high frequency harmonic vibration," *Smart Mater. Struct.*, vol. 23, no. 3, p. 35017, 2014.

[11] A. S. K. Naidu and C. K. Soh, "Identifying damage location with admittance signatures of smart piezo-transducers," *J. Intell. Mater. Syst. Struct.*, vol. 15, no. 8, pp. 627–642, 2004.

[12] Y. Y. Lim, W. Y. H. Liew, and C. K. Soh, "A Parametric Study on Admittance Signatures of a PZT Transducer Under Free Vibration," *Mech. Adv. Mater. Struct.*, vol. 22, no. 11, pp. 877–884, 2015.

[13] W. Liu and V. Giurgiutiu, "Finite element simulation of piezoelectric wafer active sensors for structural health monitoring with coupled-filed elements," in *The 14th International Symposium on: Smart Structures and Materials & Nondestructive Evaluation and Health Monitoring*, 2007, p. 65293R–65293R.

[14] S. Moharana and S. Bhalla, "Numerical investigations of shear lag effect on PZT-structure interaction: review and application," *Curr. Sci.*, vol. 103, no. 6, pp. 685–696, 2012.

[15] C.-W. Ong, Y. Yang, A. S. Naidu, Y. Lu, and C. K. Soh, "Application of the electro-mechanical impedance method for the identification of in-situ stress in structures," in *SPIE's International Symposium on Smart Materials, Nano-, and Micro-Smart Systems*, 2002, pp. 503–514.

[16] Y. Y. Lim and C. K. Soh, "Effect of varying axial load under fixed boundary condition on admittance signatures of electromechanical impedance technique," *J. Intell. Mater. Syst. Struct.*, p. 1045389X12437888, 2012.

[17] V. G. M. Annamdas, Y. Yang, and C. K. Soh, "Influence of loading on the electromechanical admittance of piezoceramic transducers," *Smart Mater. Struct.*, vol. 16, no. 5, p. 1888, 2007.

[18] A. S. K. Naidu and C. K. Soh, "Damage severity and propagation characterization with admittance signatures of piezo transducers," *Smart Mater. Struct.*, vol. 13, no. 2, p. 393, 2004.